C. R. Physique 18 (2017) 78–85

Contents lists available at ScienceDirect

Comptes Rendus Physique

www.sciencedirect.com

Energy and radiosciences / Énergie et radiosciences

Wireless energy transfer: Dielectric lens antennas for beam shaping in wireless power-transfer applications

Transfert d'énergie sans fil : antennes diélectriques pour la mise en forme des faisceaux dans les applications de transfert d'énergie sans fil

Ricardo Gonçalves [a,b,*], Nuno B. Carvalho [a,b], Pedro Pinho [b,c]

[a] *DETI, University of Aveiro, Aveiro, Portugal*
[b] *Instituto de Telecomunicações, Aveiro, Portugal*
[c] *Instituto Superior de Engenharia de Lisboa, Lisboa, Portugal*

A R T I C L E I N F O

Article history:
Available online 9 December 2016

Keywords:
Lens antennas
Wireless power transfer
3D Printing

Mots-clés :
Antennes lentilles
Transfert d'énergie sans fil
Impression 3D

A B S T R A C T

In the current contest of wireless systems, the last frontier remains the cut of the power cord. In that sense, the interest over wireless energy transfer technologies in the past years has grown exponentially. However, there are still many challenges to be overcome in order to enable wireless energy transfer full potential. One of the focus in the development of such systems is the design of very-high-gain, highly efficient, antennas that can compensate for the propagation loss of radio signals over the air.
In this paper, we explore the design and manufacturing process of dielectric lenses, fabricated using a professional-grade desktop 3D printer. Lens antennas are used in order to increase beam efficiency and therefore maximize the efficiency of a wireless power-transfer system operating at microwave frequencies in the K_u band. Measurements of two fabricated prototypes showcase a large directivity, as predicted with simulations.

R É S U M É

Dans la compétition actuelle entre les systèmes sans fil, la dernière frontière reste la coupure du cordon électrique. Dans ce sens, l'intérêt des technologies de transfert d'énergie sans fil a crû exponentiellement au cours des dernières années. Cependant, de nombreux défis à surmonter demeurent pour qu'on puisse déployer à son plein potentiel le transfert d'énergie sans fil. L'un des objectifs poursuivis dans le cadre du développement de tels systèmes est la conception d'antennes à très haut gain, très efficaces, qui permettraient de compenser les pertes liées à la propagation des signaux radio dans l'air. Dans cet article, nous explorons la conception et la fabrication de lentilles diélectriques, réalisées à l'aide d'une imprimante 3D de bureau de qualité professionnelle. Les antennes à lentilles sont utilisées en vue d'accroître l'efficacité du réseau et donc de maximiser celle d'un système de transfert d'énergie actif aux fréquences des micro-ondes dans la bande K_u. Les mesures

* Corresponding author at: Instituto de Telecomunicações, Campus Universitario de Santiago, 3810-148 Aveiro, Portugal.
E-mail address: rgoncalves@av.it.pt (R. Gonçalves).

http://dx.doi.org/10.1016/j.crhy.2016.11.004
1631-0705/

réalisées sur deux prototypes mettent en évidence une grande directivité, ainsi que les simulations le prédisaient.

1. Introduction

Wireless power transfer (WPT) is a technology that has been idealized by Nikolas Tesla more than a century ago. However, only recently the advances in technology have allowed it to become a reality. After the boom in the wireless communications in the past decades, only the power cord is left to cut in order to create truly wireless systems.

The first approach to wireless power transfer was based in inductive coupling, also referred as near-field power transfer, appearing in the toothbrushes charging systems and more recently in the form of charging pads for cell phones. This is a well-established technology; however, near-field power transfer only allows the transmission of energy in very close distances of communication. The transfer of energy over larger distances is yet a field of high interest and one that has motivated a lot of research in the past few years.

Far-field WPT is a current research topic of high interest. It is being thought of for applications to Wireless Sensor Networks (WSNs), in Radio Frequency Identification (RFID), and is a key feature for enabling the implementation of the concept of the Internet of Things [1]. More than that, WPT solutions are being considered for a wide variety of applications such as electric vehicle charging [2,3], to power up exploration probes in space [4], and for space-to-earth power transmission [5,6].

The major drawback in these systems is their efficiency in energy transfer. The wavefronts of electromagnetic waves spread in space, dissipating the energy in all directions. From this realization comes the well-known Friis transmission equation that allows the calculation of the ratio of power transmitted to power received by two antennas separated by a distance $R > 2D^2/\lambda$, being D the biggest dimensions of the antennas, which imposes that those antennas be in the far-field region of each other. The Friis transmission equation states that

$$P_\mathrm{r} = P_\mathrm{t}(1 - |\Gamma_t|^2)(1 - |\Gamma_r|^2)\left(\frac{\lambda}{4\pi R}\right)^2 G_\mathrm{t}(\theta_t, \phi_t) G_\mathrm{r}(\theta_r, \phi_r) |\hat{\rho}_\mathrm{t} \cdot \hat{\rho}_\mathrm{r}|^2 \quad (1)$$

being P_r the received power, P_t the transmitted power, Γ the reflection coefficient of the antenna, G the gain of the antenna, and $|\hat{\rho}_\mathrm{t} \cdot \hat{\rho}_\mathrm{r}|^2$ the polarization ratio.

From this relation, it is easy to realize that in order to maximize the power received, one should provide antennas that have the best matching possible, and are perfectly aligned in the direction of maximum gain to each other, as well as polarization. The hardest part is overcoming the losses due to wave-front spreading $\left(\frac{\lambda}{4\pi R}\right)^2$. To compensate this loss, very high gain antennas are needed, such as antenna arrays of several elements, parabolic antennas, or lens antennas.

Parabolic antennas have dimensions and weights that make them very difficult to integrate in many systems, even in space applications, where the size of satellites is being constantly decreased. Antenna arrays are very interesting, however, when the number of elements in the array increases, the feeding networks increase as well and the insertion losses can become quite considerable, hindering the overall gain of the antenna.

In this paper, we present the development of a dielectric lens antenna for transmission and harvesting of energy in the $\mathrm{K_u}$ band for space applications; more specifically, to be used as a transmitting source to power up passive sensors in space.

The dielectric lens is developed using 3D printing techniques, which allows the reduction of the cost, but specially to perform quick prototyping and optimization of the structures. The interest and availability of household 3D printers have increased in the past few years. Due to that, the prices of these equipments have decreased considerably. Most low-cost household 3D printers work based on the superposition of layers of a polymer material, known as thermoplastics, such as ABS (acrylonitrile butadiene styrene) or PLA (polylactic acid). These polymeric-type materials are non-magnetic dielectric and therefore can be useful for microwave applications. That has launched a new interest on this kind of technology and has incited the development of quick prototyping in many fields of science, namely electronics and including microwave circuits and antennas [7–9].

In this paper, we show the development of a 3D-printed convex paraboloid dielectric lens with a microstrip patch feed for the $\mathrm{K_u}$ band. This antenna is especially useful for WPT applications when compared to the use of antenna arrays. Arrays usually comprise a feeding network that will inevitably introduce power losses. With a lens antenna, we can, with a single-feed radiating element, achieve very high directivities, comparable to those obtained with a 16- to 20-element antenna array, without the inherent feeding network losses. The paper is organized as follows. In the following section, the dielectric lens as well as the feeding patch characteristics are described. In section 3, the simulation and measurement results are discussed. Section 4 draws the main conclusions about this work.

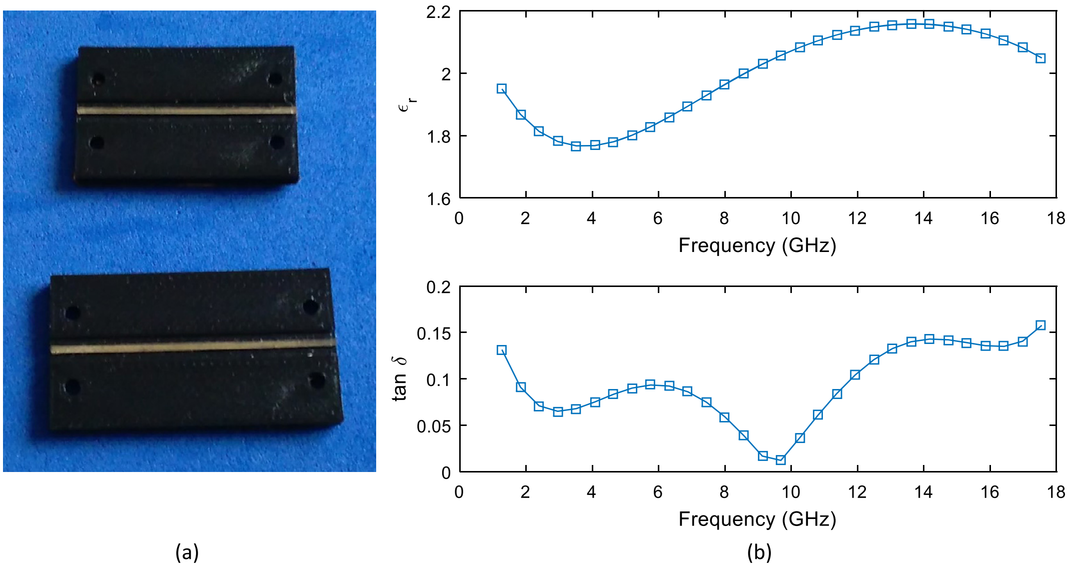

Fig. 1. Photograph of the microstrip lines on PLA substrate prototypes (a) and the estimated permittivity and dissipation factor of PLA between 1 and 18 GHz (b) using the method in [13,14].

2. Lens antenna design

Lens are used to shape wavefronts and are usually classified as dielectric lenses or constrained lenses [10]. Dielectric lenses can be hard to fabricate, requiring molds that can be expensive. This cost can be significantly lowered and the fabrication process eased and speeded if we consider 3D printing technology.

The lens shape is bound to the radiation properties one pretends to achieve. That is, the profile of the lens can be shaped in order to provide the highest gain possible (narrower beam), provide broader beams, or even be shaped to provide an isoflux-type pattern [11]. For low frequencies, the large size and weight of the lens can make its use prohibitive; it is the case when one wants to achieve very high directivities, beyond 30 dBi, for which the losses inside the dielectric of the lenses can hinder radiation efficiency. Still, lens antennas are a very attractive solution to easily manipulate the radiation shape of a given source and to create planar front waves, specially when working on high frequencies above the X-band.

The lens can have flat surfaces, in either the focal plane or the wavefront, spherical surfaces on both planes, but can also take arbitrary shapes, in order to achieve a very particular radiation shape [12]. In this particular case, we chose an ellipsoidal profile lens.

2.1. Material properties

In order to properly dimension the lens antenna and predict the antenna radiation properties, the permittivity of the dielectric used for the lens must be known in order to determine its refractive index.

The dielectric lenses proposed in this paper were fabricated with a BEEtheFirst 3D printer from BEEVeryCreative usin PLA with an infill density of 80%. Since there is no information regarding the permittivity and dissipation factors of the considered material at the frequencies of interest; these had to be determined. For that purpose, we employed a differential phase method with microstrip lines [13,14]. In order to implement this method, two microstrip lines with different lengths were fabricated using a conductive silver-based ink, which was deposited unto two slabs of PLA, as shown in Fig. 1(a).

In this method, the effective permittivity of the substrate can be related to the difference between the phase constant (β) obtained from the propagation constant (γ) of the lines and the propagation phase in the vacuum (β_0) as

$$\varepsilon_{\mathrm{r,eff}} = \left(\frac{\beta}{\beta_0}\right)^2 \tag{2}$$

where the propagation constant of the lines is obtained by solving the following eigenvalue equation

$$\lambda_{1,2} = \frac{1}{2}\left[\mathrm{Tr}(M) \pm \sqrt{\mathrm{Tr}(M)^2 - 4\Delta M}\right] \tag{3}$$

where $\mathrm{Tr}(M)$ is the trace and ΔM is the determinant of M, being M the transmission matrix corresponding to the section of line difference between the two transmission lines. Since it is a transmission matrix it is the direct ratio between the transmission matrix of each line

$$\bar{M} = \bar{M_1} \cdot \bar{M_2}^{-1} \tag{4}$$

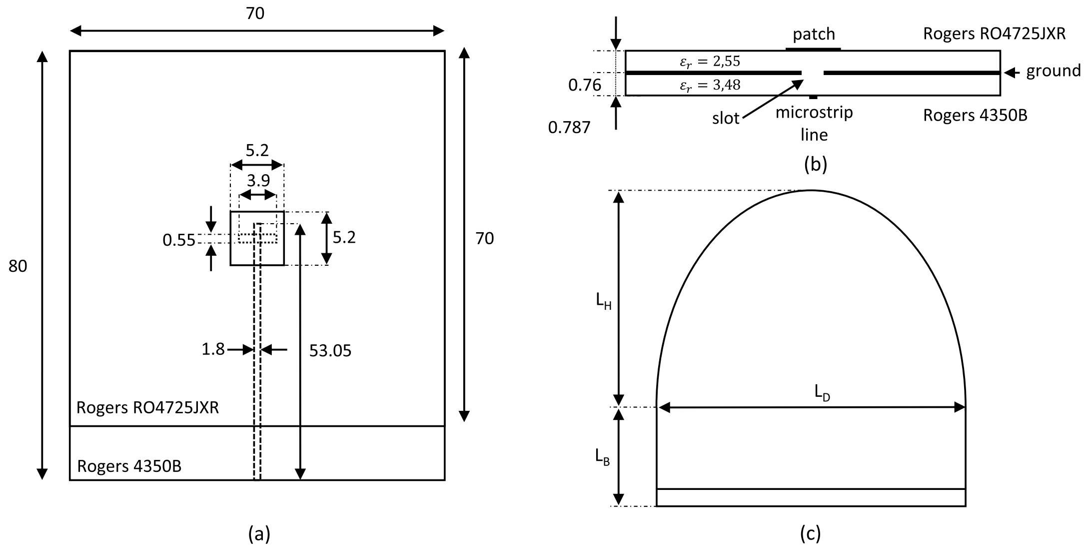

Fig. 2. Schematic of the proposed antenna (a) top view of the slot coupled microstrip patch antenna, (b) profile view, and (c) lens profile characteristics.

and this can be obtained from the measured S-parameters as

$$M_i = \frac{1}{S_{21i}} \begin{bmatrix} (S_{12i}S_{21i} - S_{11i}S_{22i}) & S_{11i} \\ -S_{22i} & 1 \end{bmatrix} \tag{5}$$

Since the system is passive, the relation $|e^{-\gamma \Delta l} < 1|$ imposes a particular signal for the solution of (3). The propagation constant can then be defined as

$$\gamma = \frac{1}{\Delta l} \ln \lambda_{av} + j \frac{2\pi n}{\Delta l} \tag{6}$$

being $\lambda_{av} = \frac{1}{2}\left(\lambda_1 + \frac{1}{\lambda_2}\right)$ the average of the solution of (6); if $\Delta l < \lambda_0 2$, then $n = 0$.

The results obtained from the application of the referenced method are depicted in Fig. 1, and the permittivity estimated at 13.5 GHz is 2.16.

As can be seen from the results in Fig. 1, permittivity exhibits a strange behavior with frequency. An increase in permittivity is expected; however, it decreases for the lowest frequencies and again for the higher frequencies, this is rather unexpected. Therefore, we used the characterization technique as proposed in [15] in order to confirm the permittivity of the PLA material at frequencies close to 13.5 GHz. The obtained value was $\varepsilon_r = 2.04$, which is lower than the value calculated with the previous method.

Considering these results, we used a relative permittivity of $\varepsilon_r = 2.0$ to model the lens material during simulations. This value has proven to be accurate considering the measured results shown in the following sections.

The dissipation factor determined with the first method presents an awkward behavior; therefore, the values obtained were not considered. Instead, we considered a dissipation factor of $\tan\delta = 0.01$. This value has little effect on the input impedance of the antenna, and mainly influences radiation efficiency. Therefore, by comparing the simulated and measured gain, we could conclude about the real loss factor, which is discussed further.

2.2. Antenna design

The lens antenna is fed by a microstrip patch antenna. In order to feed the lens with a symmetrical electric field and to avoid interference that could disrupt the radiation pattern, we used a slot-coupled fed microstrip patch, as shown in Fig. 3(a). The use of the slot coupled microstrip patch, as opposed to a microstrip line fed patch, isolates the feed line and the patch electric fields, preventing leakage radiation from the line to feed the lens and therefore disturbing the radiation pattern.

The dimensions of the slot-coupled microstrip patch antenna are presented in Fig. 2, along with the lens schematic profile. A photograph of the prototypes is shown in Fig. 3, and the dimensions of the two lenses are described in Table 1.

The shape of the radiation beam depends on the curve profile of the lens and the ellipsoidal profile is a natural evolution of the hemispherical lens in order to maximize the directivity while keeping the same lens base diameter. The profile of the lens is obtained from the following expression

$$y = h\sqrt{1 - \frac{x^2}{r^2}} \tag{7}$$

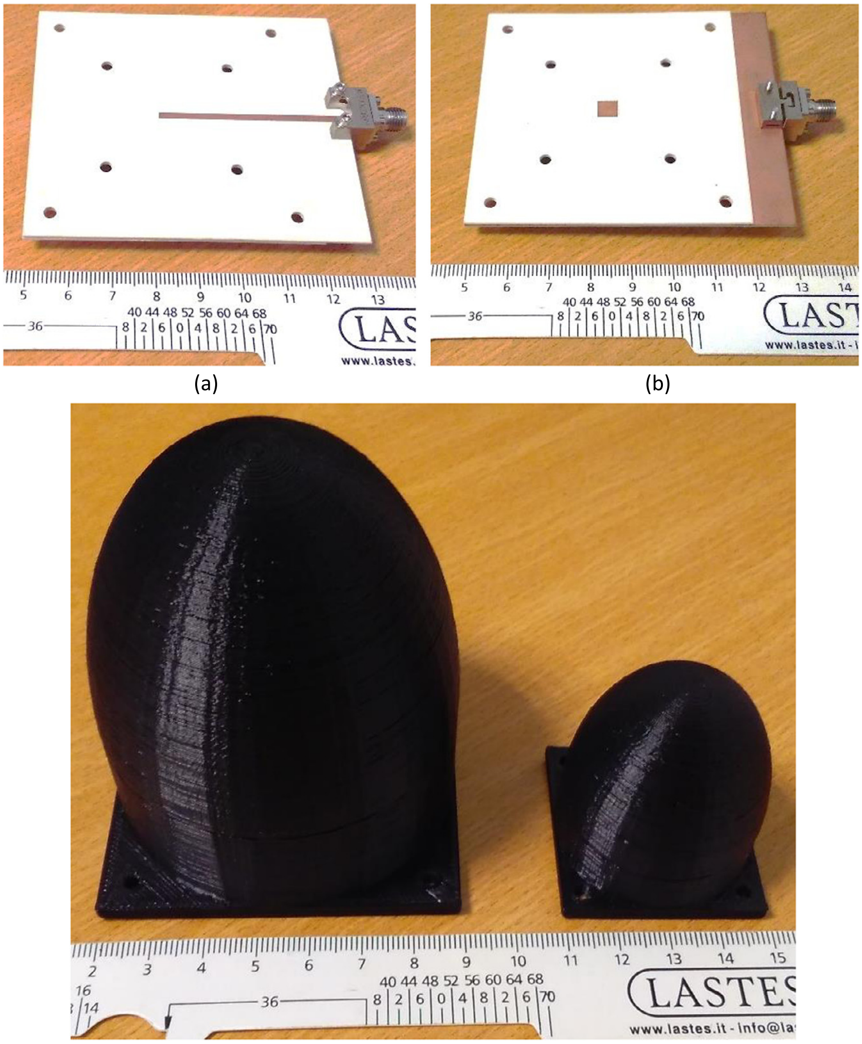

(c)

Fig. 3. Photograph of the built prototypes: (a) bottom side of the slot-coupled microstrip patch antenna, (b) top side of the microstrip patch antenna, and (c) lens antenna prototypes.

Table 1
Lens antenna dimensions and weight.

	Lens 1	Lens 2
L_{H} (mm)	58.9	33.0
L_{B} (mm)	29.0	15.0
L_{D} (mm)	35.0	20.0
Weight (g)	245	43

being h the height of the lens (L_{H}) and r is the radius of the lens base ($L_{\mathrm{D}}/2$). The length of the cylindrical extension is obtained according to geometrical optics rules [16], and it should be $L_{\mathrm{B}} = L_{\mathrm{H}} \times n$, where n is the refractive index of the lens.

After defining the profile that could maximize directivity considering a given diameter for the lens, we increased the diameter of the lens in order to study the improvement in terms of directivity versus the overall size of the lens. It is important to note that the increase in size of the lens increases directivity; however, the dielectric used for the lens has losses, therefore these can hinder the radiation gain of the antenna.

In order to evaluate the behavior of the lens antennas and the compromise between size, weight and overall radiation gain, two prototypes for the lens antenna were built, while using the same microstrip patch antenna for feeding.

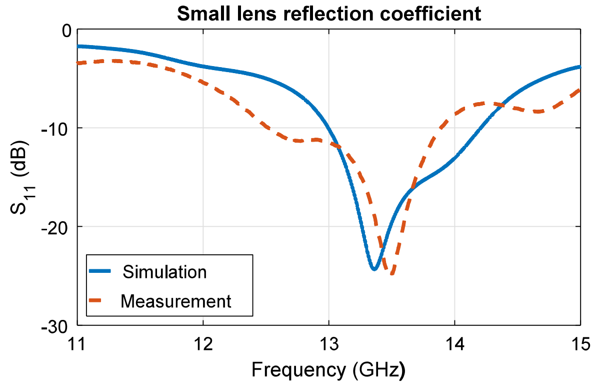

Fig. 4. Simulated and measured reflection coefficient of the small-lens antenna.

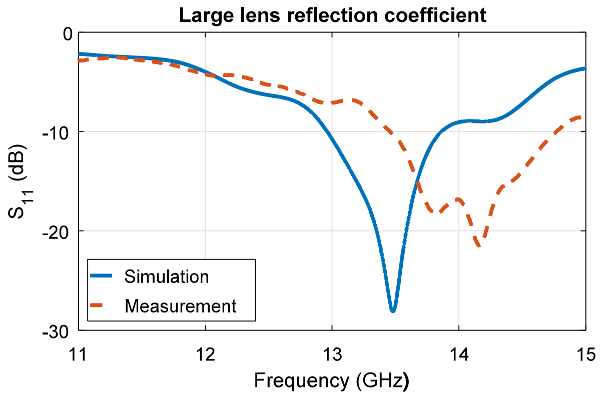

Fig. 5. Simulated and measured reflection coefficient of the large-lens antenna.

3. Antenna characteristics

The microstrip patch antenna used to feed the lens is considerably influenced by the superposition of the dielectric material; therefore, its dimensions as well as the coupling slot and the stub are designed in order to match its input impedance, at the desired frequency, considering the dielectric lens attached to it. For that reason, the reflection coefficient of the microstrip patch is non-relevant without the presence of the lens.

According to simulations, the reflection coefficients of the microstrip patch with the two lenses is not very different, as can be seen in the simulation curves presented in Fig. 4. However, as can be seen from the results in Figs. 4 and 5, the measured reflection coefficient of the antenna with the larger lens presents a shift in frequency when compared to the smaller lens measurements and when compared to the simulation curves. This can be explained by some warping effects that occurred during printing. Since the larger lens is a rather big and heavy object, it is very difficult to keep the whole surface on the printing table during the whole process, therefore creating some warping in the edges. Even after sanding the bottom surface, there is always a little warping around the corners of the structure; this causes the microstrip patch board to bend on the edges when screwed together with the lens. We believe that this is the cause for the shift in frequency occurring in the measurements, which is not observable in the simulations. Two lens were printed, the second one at a lower speed, but the warping problem has proved difficult to overcome. Nevertheless, the results are satisfactory, since we can always re-tune the feeding antenna if the larger lens is selected.

The simulated versus measured normalized radiation pattern obtained with the lens is depicted in Fig. 6.

The agreement between simulation and measurement for both lens antenna prototypes in both measured planes is clear. In most cases, the HPBW difference between simulation and measurement was less than 1°, with an exception for the small lens in the XZ plane with a difference of 4.5°.

As stated before, the change in the lens curvature as well as the increase in the lens size will increase its directivity, but also hinder the efficiency due to dielectric losses. The maximum simulated directivity for the small lens was 14.7 dBi, with a radiation efficiency of 75.9%, which translates in a gain of 13.6 dBi, which is close to the 14.1 dBi measured. The maximum simulated directivity for the large lens was 18.7 dBi, with a radiation efficiency of 66.1%, which translates in a gain of 16.0 dBi, which is close to the 16.4 dBi measured.

The fact that we measured higher gains than the simulated ones proves that the dissipation factor of the dielectric material is actually lower than the one considered during initial simulations. We performed a parametric sweep in order

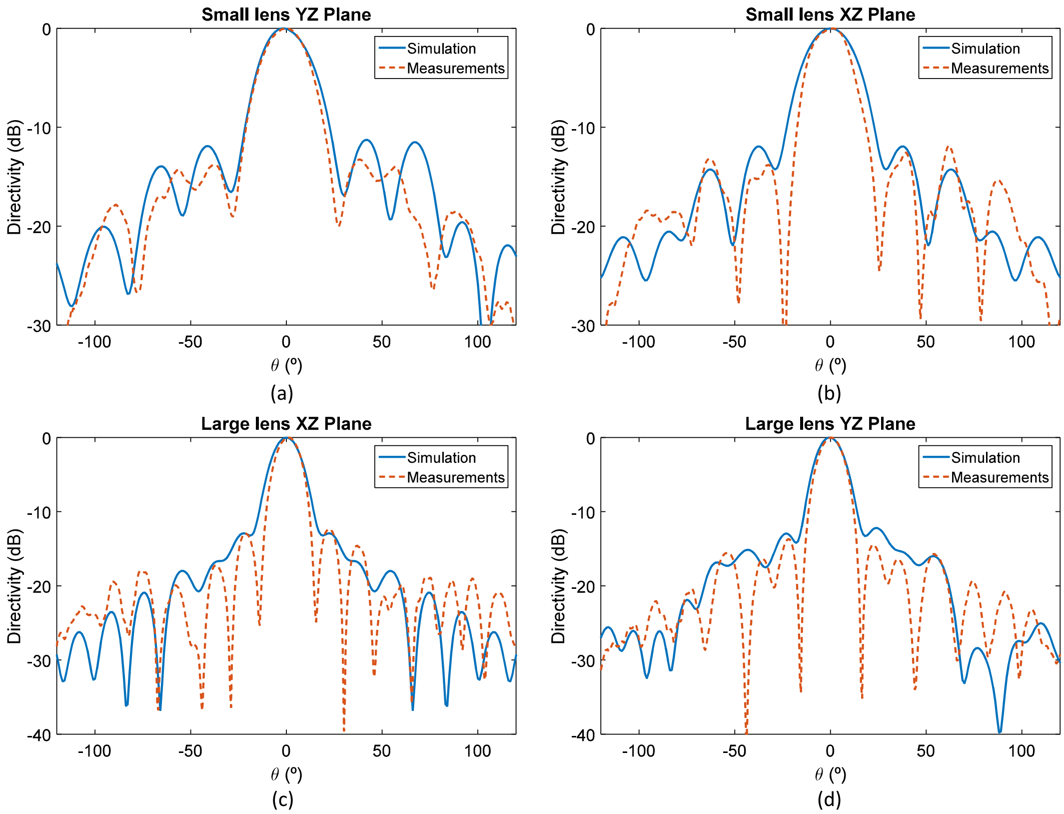

Fig. 6. Simulated and measured normalized radiation pattern of (a) the XZ plane of small lens, (b) the YZ plane of the small lens, (c) the XZ plane of the large lens antenna, and (d) the YZ plane of the large lens.

to find which dissipation factor would approximate the measured gain at best, reaching an actual dissipation factor of $\tan\delta = 0.005$.

4. Conclusion

Lens antennas are particularly useful for frequencies above the X band to create narrow-beam and high-gain wireless transmission systems. The prototypes described in this paper prove that 3D printing technology can be a very useful tool to create dielectric structures, in this case dielectric lenses, but can be extended to dielectric resonators. The utility that one can get from a 3D printer is immense, the infill manipulation can be useful to shape dielectric structures for radiation shaping such as Luneberg or Fresnel lenses.

The antennas proposed in this paper exhibit a high radiation gain, which is rather useful for, but is not limited to, applications to wireless power transfer. When compared to antenna arrays, this approach has the advantage of discarding the use of complex feeding network that have inherent transmission losses, therefore increasing the transmitted power. There is, however, a compromise between the gain and the size and weight of the lens; therefore, depending on the gain levels one pretends to reach, the viability of a lens antenna has to be carefully assessed. Therefore, dielectric lens antennas can prove to be a solution for very high-gain antenna design for wireless energy transfer systems.

References

[1] L. Roselli, N.B. Carvalho, F. Alimenti, P. Mezzanotte, G. Orecchini, M. Virili, C. Mariotti, R. Gonçalves, P. Pinho, Smart surfaces: large area electronics systems for internet of things enabled by energy harvesting, Proc. IEEE 102 (11) (2014) 1723–1746, http://dx.doi.org/10.1109/JPROC.2014.2357493.

[2] N. Shinohara, Y. Kubo, H. Tonomura, Wireless charging for electric vehicle with microwaves, in: Proc. 3rd International Electric Drives Production Conference, EDPC, 2013, pp. 1–4.

[3] N. Shinohara, Y. Kubo, H. Tonomura, Mid-distance wireless power transmission for electric truck via microwaves, in: Proc. URSI International Symposium on Electromagnetic Theory, EMTS, 2013, pp. 841–843.

[4] S. Kawasaki, Microwave WPT to a rover using active integrated phased array antennas, in: Proc. 5th European Conference on Antennas and Propagation, EUCAP, 2011, pp. 3909–3912.

[5] H. Matsumoto, Research on solar power satellites and microwave power transmission in Japan, IEEE Microw. Mag. 3 (4) (2002) 36–45, http://dx.doi.org/10.1109/MMW.2002.1145674.

[6] N. Shinohara, Beam control technologies with a high-efficiency phased array for microwave power transmission in Japan, Proc. IEEE 101 (6) (2013) 1448–1463, http://dx.doi.org/10.1109/JPROC.2013.2253062.

[7] A. Bisognin, D. Titz, F. Ferrero, R. Pilard, C.A. Fernandes, J.R. Costa, C. Corre, P. Calascibetta, J.M. Rivière, A. Poulain, C. Badard, F. Gianesello, C. Luxey, P. Busson, D. Gloria, D. Belot, 3D printed plastic 60 GHz lens: enabling innovative millimeter wave antenna solution and system, in: IEEE MTT-S International Microwave Symposium, IMS2014, 2014, pp. 1–4.
[8] K. Gbele, M. Liang, W.R. Ng, M.E. Gehm, H. Xin, Millimeter wave Luneburg lens antenna fabricated by polymer jetting rapid prototyping, in: 39th International Conference on Infrared, Millimeter, and Terahertz Waves, IRMMW-THz, 2014, pp. 1.
[9] S. Zhang, Design and fabrication of 3D-printed planar Fresnel zone plate lens, Electron. Lett. 52 (10) (2016) 833–835, http://dx.doi.org/10.1049/el.2016.0736.
[10] J.J. Lee, Antenna Handbook, vol. II, Chapter 16, Van Nostrand Reinhold, 1993.
[11] J.R. Costa, C.A. Fernandes, G. Godi, R. Sauleau, L.L. Coq, H. Legay, Compact ka-band lens antennas for LEO satellites, IEEE Trans. Antennas Propag. 56 (5) (2008) 1251–1258, http://dx.doi.org/10.1109/TAP.2008.922690.
[12] R. Sauleau, B. Bares, A complete procedure for the design and optimization of arbitrarily shaped integrated lens antennas, IEEE Trans. Antennas Propag. 54 (4) (2006) 1122–1133, http://dx.doi.org/10.1109/TAP.2006.872563.
[13] M.D. Janezic, J.A. Jargon, Complex permittivity determination from propagation constant measurements, IEEE Microw. Guided Wave Lett. 9 (2) (1999) 76–78, http://dx.doi.org/10.1109/75.755052.
[14] F. Declercq, I. Couckuyt, H. Rogier, T. Dhaene, Environmental high-frequency characterization of fabrics based on a novel surrogate modelling antenna technique, IEEE Trans. Antennas Propag. 61 (10) (2013) 5200–5213, http://dx.doi.org/10.1109/TAP.2013.2274031.
[15] R. Goncalves, R. Magueta, P. Pinho, N.B. Carvalho, Dissipation factor and permittivity estimation of dielectric substrates using a single microstrip line measurement, Appl. Comput. Electromagn. Soc. J. 31 (2) (2016) 118–125.
[16] X. Wu, G.V. Eleftheriades, T.E. van Deventer-Perkins, Design and characterization of single- and multiple-beam mm-wave circularly polarized substrate lens antennas for wireless communications, IEEE Trans. Microw. Theory Tech. 49 (3) (2001) 431–441, http://dx.doi.org/10.1109/22.910546.